Deducing Function through Localization: PCV1 VP3 the Problem Child

A Major Qualifying Project Submitted to the Faculty of

WORCESTER POLYTECHNIC INSTITUTE

In partial fulfillment of the requirements for the

Degree of Bachelor of Science

By

Daniel C. Millard
Biochemistry and Biotechnology

Philip P. Economou
Biochemistry

Abstract

The harmful side effects of many existing cancer interventions, along with the variety of mutations a given cancer may have, underscore a need for specific and novel treatments. The Circoviridae family of viruses have several members that encode proteins observed to induce apoptosis in human cells with specificity towards cancer cells. One unique example, PCV1-VP3, has significant morphological and functional differences with its homologues, possessing an additional tail domain and localizing in the cytoplasm rather than the nucleus of transformed cells. Previous investigations have focused largely on the identification of a nuclear export sequence, and have yielded inconclusive results. To gain insight into possible mechanisms of action, compartmentalization of PCV1-VP3 was investigated using differential detergent fractionation and fluorescent microscopy. Results suggest colocalization with the endoplasmic reticulum, potentially identifying pathways to target in future investigations.

Table of Contents

Table of Tables and Figures

Acknowledgements

In reflecting on this project, we would like to thank those who have made our involvement in this research possible through their help. It is through the guidance and feedback of our advisers Professor Destin Heilman and Professor Tanja Dominko, that our research aims and methods were formulated and implemented, and the results of which were analyzed. We also find it important to recognize the research of Professor Heilman and previous student research in his lab on PCV1 VP3 upon which our endeavors are based. The efforts of Silvana Reid, the Heilman lab manager, were also critical for ensuring the availability of necessary laboratory supplies, and the assistance of Vicki Huntress in operating the confocal microscopy was instrumental in our microscopy experiments. It is through the support of all those responsible for our progress that we have been able to grow as scientists building technical and mental skills that will be critical in our careers moving forward. To those mentioned above and those that may not have been listed, thank you.

Introduction

Cancer is a disease characterized by excessive cell growth, with potential to occur in a wide variety of cell and tissue types. This aberrant growth impairs function of the implicated tissues, ultimately resulting in organ failure and subsequently death. Although a single mutation may be responsible for the initial creation of cancerous cells (often caused by external factors such as pathogens, chemicals, or radiation), multiple built-in checkpoints for cell growth must be supplanted for the disease to progress, necessitating multiple mutations. Mutations are developed at an increasing rate as cancerous cells grow in number and divide more rapidly.

In addition to regulatory checkpoints, a prospective cancer cell must overcome the Hayflick limit, the maximum amount of divisions a cell population can undergo before death. This is primarily influenced by the shortening of telomeres during each replication cycle. To reach senescence, the cell must mutate such that telomerase, the enzyme responsible for building telomeres in gametes, is reactivated . This renders a cell immortalized, but not yet tumorigenic. Further changes must be accrued to make these otherwise normal cells divide rapidly and behave atypically, disrupting normal tissue function and posing a threat to the organism (1).

These cells have several morphological characteristics that distinguish them from healthy cells, and reflect important biochemical differences (2). For example, their nuclei are often larger and more elongated than is typical. This is a result of increased production of regulatory proteins that are necessary to sustain rapid cell growth, which build up in the nucleus and distort chromatin. The nuclear margin has been shown to thicken due to buildup of transcriptionally inactive chromatin. Several other nuclear distortions have been observed with similar root causes (3), including the presence of grooves and invaginations (inside-out regions that form

tunnel-like structures). Outside the nucleus, the highly active metabolism of cancer cells leads to increased levels of RNA, making the cytoplasm basophilic. Mitochondria can become abnormal in size and shape, generally decreasing in number. Cells can also exhibit anaplasia, a loss of differentiation that is correlated with poorly developed golgi bodies in transformed cells. This phenomenon occurs mostly in highly malignant cancers, and some evidence suggests this plays an important role in cancer cells' ability to invade highly differentiated tissue (3).

A persistent challenge in the development of cancer treatments when surgery is not a viable option is the relative similarity that cancer cells (transformed cells) have to healthy cells. Many existing strategies, such as certain chemotherapies, exploit the increased need that transformed cells have for resources due to their rapid growth, thus affecting such cancerous cells more rapidly than healthy cells. Healthy cells are still damaged, albeit at a slower rate, introducing side effects and making treatment a potentially difficult experience for the patient. Other strategies take advantage of existing mechanisms for apoptosis (programmed cell death) triggered by DNA damage to increase specificity, but these treatments are often not applicable on a case-by-case basis. It is possible that a mutation effectively disabling a given pathway for apoptosis has already been accrued by the cancer. One such pathway is p53, an important and well-characterized tumor suppressor involved in cell cycle arrest, DNA repair, and apoptosis (4,5). Thus, additional methods to target cancer cells with specificity are desirable in the continued development of cancer treatments.

The *Circoviridae* Virus Family

The association between viruses and cancers has grown in recent years as it is now known that certain viruses may even directly cause oncogenesis, such as has been found with the Human Papillomavirus (6). These viral pathogens gain their infective capabilities from highly

selective receptors on their protein coat as well as their ability to overtake a host cell's metabolism. As such, research efforts have been made to utilize their machinery in highly specific and delicate medical procedures, such as gene therapy and cancer treatment. After decades however, these efforts have found limited overall success, and direct treatment with viral loads has become contested by many as unsafe due to incidences of strong immune responses leading to patient death in some cases (7). Because of this, other avenues have been explored to harness these mechanisms and viral strains with antitumor behavior, notably certain members within the *Circoviridae* family, have become of keen interest.

The *Circoviridae* family are characterized by ambisense genomes made of circular, covalently closed, single-stranded DNA (ssDNA) ranging from 1.7 to 2.1kb and are divided into the *Circovirus* and the *Cyclovirus* genera. This classification is based upon genome organization, particularly the relative distances between the origin of replication and at least two open reading frames (ORFs) coding for the replication-associated protein and the capsid protein (8). Including some of the smallest known viral pathogens, members of the *Circovirus* genus infect a wide range of vertebrates including birds and mammals and have been studied for their agricultural impacts (9,10). Most notably, however, certain members of this genus have been identified for producing proteins capable of causing apoptosis in transformed carcinoma cells, while leaving healthy cells intact (11). Among these, the chicken anemia virus (CAV) in particular has been extensively studied for its selective apoptotic effect. Observed in nature to hinder chicken development and growth, this virus infects mitotic cells often leading to significant growth abnormalities and even death (12).

Like many other members of the *Circoviridae* family, the CAV genome contains three ORFs, each coding for proteins necessary for virus pathology. The third of these ORFs codes

for Apoptin, the apoptotic agent responsible for cell lysis and the subsequent release of new virus particles. Interestingly, when expressed in mammalian systems this protein exhibits selective apoptosis, seemingly differentiating between primary and cancerous cells (12). Through mechanisms that are still contested, Apoptin appears to function in the nucleus to activate pathways that interrupt the cell cycle and initiate caspase signalling pathways associated with programmed cell death (13,14). Specifically, the protein has been shown to associate with the APC1 subunit of the anaphase-promoting complex (APC), leading to G2/M cell cycle arrest. This explains the relevance of nuclear localization in transformed cells, but not its precise mechanism, as Apoptin is cytoplasmic in primary cells. Correspondingly, the C-terminal nuclear export signal (NES) appears weaker in transformed cells, allowing the N-terminal nuclear localization sequence (NLS) to take precedence and Apoptin to concentrate in the nucleus. Notably, this specificity in localization is not observed in Apoptin homologs, despite the apparent importance to its mechanism (13).

Importantly, these pathways operate independently of the ubiquitous p53 tumor suppressor, a common anticancer target valid in 50% of cases for a given cancer at best (13,15). In addition, the apoptotic pathway utilized has been shown to be intrinsic, activating caspase 3 via release of cytochrome C from mitochondria. This is an advantageous target for treatment over extrinsic pathways, which require extracellular signaling and therefore increase the risk of non-specific apoptosis. Given the potential for Apoptin to not only reveal novel apoptotic pathway targets in cancer, but to also be used directly as a therapeutic, various studies have begun testing viral delivery methods to cancerous cells (16,17).

Following much of the same genetic organization as CAV, the porcine circoviruses (PCV) are also *Circoviridae* family members possessing at least three ORFs and observed anti

tumor activity. Of these, there are at least three distinct types each responsible for pig infections of widely ranging consequence. The recently discovered PCV3 strain along with PCV2a + b in particular are known to be responsible for multiple porcine afflictions including porcine dermatitis and nephropathy syndrome (PDNS), failed pregnancy, and postweaning multisystemic wasting syndrome (PMWS) (18, 19). These pathologies, collectively grouped as the porcine circovirus diseases (PCVD) are caused by the virus' apoptotic ability. As in the case of CAV, the proteins coded for by the third ORF in their respective virus genomes are largely responsible for cell lysis, though other potential proteins may also be involved at least in the case of PCV2 (20). Like CAV's Apoptin, the PCV1 and 2 Virus Protein 3s (VP3s) have also been shown to have peculiar apoptotic behavior, selectively lysing various established carcinoma models such as the H1299 non-small cell lung carcinoma cell line.

Given the novelty of PCV3, there appears to be little data in the literature regarding its biochemical mechanisms in either porcine or human models and its potential for selective apoptosis of cancer cells. Considerable research, however, has been directed at identifying the underlying pathways for PCV2 VP3 function. Such endeavors have yielded mixed results. Early data indicated the protein functions to activate caspase-8 and -3 pathways to induce apoptosis in PK15 cells (porcine kidney cells) (21) and to similarly activate caspase-3/7 pathways in H1299 cells (22). Interestingly, other studies utilizing a pan-caspase inhibitor reaffirmed PCV2 VP3 to induce apoptosis via a caspase-3 dependent manner in PK15 cells and, contrastingly, in a caspase-8 and -3 independent manner in B16F10 cells, a murine melanoma cell line (23). Such differences highlight potential differences between cellular models that should be kept in mind when collecting further data as even further research into PCV2 VP3's function in PK15

cells indicated apoptosis via an unfolded protein response (UPR) that has yet to be reported in tumor models (24).

Previous PCV1 VP3 Research

Alternatively to PCV2 and 3, PCV1 is largely accepted as a nonpathogenic virus in the vast majority of cases where it is found in asymptomatic pigs (25). This virus of nearly identical genome size to PCV2 (~1760nts) has also become of interest due to its peculiar biochemistry. While also displaying selective apoptotic ability, various studies have revealed PCV1 VP3 behavior to significantly differ from that of the better characterized Apoptin indicating a different mechanism of action that may also be p53 independent and provide a novel cancer target. Upon immediate comparison, such differences may be attributed to a large hydrophobic region on the C-terminus of PCV1 VP3 not present in either PCV2 VP3 or Apoptin and nearly doubling its respective length (205 a.a.) (26).

General fluorescence microscopy experiments utilizing Apoptin and PCV1 VP3 conjugated to EGFP on their N-termini have revealed fundamental differences in subcellular localization between the two proteins in transfected primary and transformed cell lines. Such investigations have revealed that Apoptin localizes to the nucleus prior to the apoptosis of transformed cells and that this localization is required to maintain function. Contrastingly, PCV1 VP3 has been observed to be strongly cytoplasmic in both primary and transformed cells even though it contains clusters of sequence homology with Apoptin at known localization sequences. This observed difference in localization along with the perplexing C-terminal hydrophobic region only known to exist in PCV1 VP3 has served as the inspiration for various mutational studies aimed at deducing the functional regions of the curious VP3 (26).

A major component of these mutational studies focused on truncation experiments to discern the general regions within the PCV1 VP3 protein and their respective functions. Preliminary truncation experiments detailed the “core” protein region (a.a. 1-105), which retains high structural homology with other circoviridae VP3s, and the hydrophobic, highly helical “tail” protein region (a.a. 105-205) thought to be unique to PCV1 VP3. Following expression in H1299 cells, it was observed that the “core” domain was strongly nuclear, like Apoptin, but lacked apoptotic ability. Even more interestingly, it was revealed that the “tail” domain retained an apoptotic effect and was strongly nuclear, retaining an expression pattern resembling the wild type protein. These results corroborate with sequence analysis conducted on PCV1 VP3, which predicted nuclear export sequences (NES) around residues 42-49, 127-136, and 134-149, placing more export potential in the “tail” region. Similar bioinformatic applications did not yield strong predictions for nuclear localization sequences (NLS), though a potential NLS was predicted around residues 80-105. Even without the presence of a well characterized NLS, however, the strongly nuclear nature of the “core” truncation indicates the presence of one in this region (26).

Continuing with this method, the “core” domain was divided into two new trunctations, a.a. 1-63 and a.a. 64-105, which contain the predicted NES and NLSs respectively. In a total curve ball, both constructs localized to the nucleus, bringing into question that accuracy of the sequence predictions. Since these predictions alone would place the a.a. 1-63 construct in the cytoplasm and the a.a. 64-105 construct in the nucleus, these results indicate that they cannot be completely responsible for the subcellular behavior of the “core” region if they are even active at all (27). Subsequent experiments created a.a. 64-205 (27) and a.a. 105-139

truncations which both produced the characteristic cytoplasmic localization pattern of the wild type, strongly indicating the NES to be located within residues 105-139 (28).

Results such as these then served as the inspiration for precise point mutational studies aimed at disrupting PCV1 VP3 localization to determine the specific residues responsible for its subcellular behavior. These studies created a multitude of mutants, such as Δ46–49 (LLHL -> AAHA) (22), Δ134–136 (LHL->AHA) (30), and Δ140–142 (LLL->AAA) (29) as well as combinations of these, designed to inhibit leucine interaction with other proteins (29, 30). Leucine specifically was targeted because of its ability to interact with chromosome region maintenance 1 (CRM1), a main nuclear export protein possibly involved in PCV1 VP3 metabolism. All of these mutants failed to disrupt the viral protein's localization indicating that additional residues other than leucine may be involved in an uncharacterized NES not involving CRM1 (29, 30). As such, mutants Δ115–117 (ILL->AAA), Δ121–126 (FFLV->AAAA) (31), and Δ113–114 (FF->TT) (28) as well as various combinations of these and previous mutations were created to target additional residues. By substituting these residues for similar residues of smaller size it was hoped that the overall protein folding would not be compromised while interfering with NES function. These mutants also failed to disrupt PCV1 VP3's localization, and while there is strong evidence for a NES between a.a. 105-139, the exact sequence responsible remains unknown and it is possible that other residues outside this region may be involved (31, 28).

Since the 149th residue is leucine, potentially interacting with CRM1, truncation mutant a.a. 1-149 as well as deletion mutant Δ105–149 (30) were created to test whether any residues outside the a.a. 105-149 region were responsible for cytoplasmic localization. While truncation a.a. 1-149, containing the predicted NES, was then shown to accumulate in the cytoplasm,

mutant Δ105–149, lacking the predicted NES, accumulated in the nucleus. These results revealed the a.a. 105-149 sequence to be critical for wild type localization and to definitely contain an NES (32).

Since in previous research only cytoplasmic PCV1 VP3 and its components have been observed to induce apoptosis, the NLS from simian virus 40 (SV40) was fused to the N-terminus of PCV1 VP3 to effectively force the protein into the nucleus. Initial killing assays have shown this fusion construct to have impared apoptotic abilities, indicating its localization outside of the nucleus to be critical to its function, though further experimentation is needed to confirm this (unpublished data). Multiple studies have also indicated that like Apoptin, PCV1 VP3 activates a caspase 3/7-dependent pathway leading to apoptosis, though its methods of doing so remains elusive and is likely different from that of the aforementioned protein (26,33). Additional research has also observed PCV1 VP3 to cause G1 cell cycle arrest, further differentiating the physiological manifestation of PCV1 VP3's mechanism of action from that of Apotin (26).

Trying a Different Approach

PCV1 VP3's unknown function in vivo makes it an attractive target of study for identifying novel anti-cancer pathways. With the ultimate goal of emulating this protein's biochemistry with a small molecule drug, researchers have struggled to find conclusive evidence for how it may operate. Previous research has relied heavily on truncation experiments to break down PCV1 VP3's modular functions. Such efforts have managed to identify potential nuclear export and localization sequences and the general regions responsible for apoptosis. A major focus in these experiments has been the large hydrophobic tail region present on the C terminus of PCV1 VP3. This region has been observed in neither Apoptin nor PCV type 2, a pathogenic PCV subtype, and roughly doubles the size of PCV1 VP3 relative to its aforementioned

relatives. These previous experiments have revealed valuable information regarding PCV1 VP3's functional regions and have highlighted its differences from related viruses but have yet to determine its mechanism of action (26, unpublished data). As such, alternative approaches to further characterize how this protein operates may be valuable and are the basis for this research. Cellular localization studies have been chosen since PCV1 VP3's functional destination in the cell is unknown and may reveal critical insights for its selective apoptosis of cancerous cells.

Materials and Methods

Primer Designs and Sequences for PCR Cloning of EGFP-PCV1 VP3

PCR was conducted with 10uL 2x GoTaq Green MasterMix, 1uL each of forward and reverse primer (1.5pmol/uL), 1uL EGFP-PCV1 VP3 parental plasmid (135pg/uL), and 7uL nuclease-free deionized H2O. Reactions consisted of an initial denaturation step at 95 degrees centigrade for four minutes, 30 amplification cycles (95 degrees centigrade for 30 seconds, 55 degrees for 30 seconds, and 72 degrees for 3 minutes), and a final extension cycle at 72 degrees centigrade for 4 minutes followed by incubation at 10 degrees before storage at -20 degrees centigrade.

Table 1. Primers for PCR Cloning of EGFP-PCV1 VP3. Green indicates the BmtI and AgeI restriction sequences located in the forward and reverse primers respectively. Blue represents the EGFP primers encompassing the EGFP-PCV1 VP3 gene construct.

Forward Primer	5'-GCTAGCATGGTGAGCAAGGGCGAG-3'
Reverse Primer	5'-ACCGGTTTATCTAGATCCGGTGGATC-3'

Transformation of Competent E. coli

Gibson Assembly or T4 Ligation products (2uL) were pipetted onto JM109 competent cells (50µL, >108cfu/µg, Promega cat. L2001). Cells were then incubated on ice for 30 minutes, heat-shocked at 37°C, and incubated on ice again for 2 minutes. Cells were then added to separate 0.45mL SOC broth and incubated for at least one hour at 37°C, 220rpm. xuL (most commonly 50-75uL) of the resulting liquid culture was then pipetted onto LB plates prepared with 50ug/mL ampicillin and allowed to grow overnight.

Colony Selection, Overnight Cultures, and Plasmid Miniprep

Isolated colonies were selected from overnight plates with transformed JM109 cells. Using a pipette tip, colonies were transferred to 2mL LB or SOC broth with 50ug/mL ampicillin

and allowed to incubate overnight at 37°C, 220rpm. The PureYieldTM Plasmid Miniprep System (Promega) was then utilized to isolate plasmid from the transformed JM109 cells following the published protocol (34).

Restriction Digests

All restriction digests were conducted with 1uL AgeI HF and/or 1uL BmtI HF, 5uL Cut Smart NEBuffer, xuL DNA construct (1ug DNA), and xuL nuclease-free DIH2O (add to 50uL total reaction mixture). Reactions were run at 37°C for >= 1 hour and stopped by either adding 10uL 6X gel loading dye or by incubation at 65°C for 20 minutes. Restricted products were then run on a 0.9% agarose gel at 90V for 40 minutes to assess restriction success and isolate DNA fragments for purification.

Post Electrophoresis or PCR DNA Purification

Following PCR to create the PCV1 VP3 insert or the restriction digest of either the PCV1 VP3 insert or pCW57.1, the Promega Wizard SV Gel and PCR Clean-up System was utilized to purify the resultant DNA products. Purification was conducted following the published protocol with both the Membrane Binding Solution and the Elution Buffer preheated to 65 degrees centigrade (35). In the case of gel purification, excised bands were incubated in Membrane Binding Solution for at least 30 minutes.

Plasmid Ligations

All Gibson Assembly ligations were conducted with 10uL Gibson Assembly Master Mix (New England Biolabs), xuL DNA (0.02-0.5pmol DNA), and xuL nuclease-free deionized H2O (add to 20uL total reaction mixture). Reactions were run at 50°C for 15 minutes.

Tissue Culture and Transfections

Human lung carcinoma cells (NCL-H1299) were cultured in Dulbecco's Modified Eagle Medium, to which 10% fetal bovine serum was added. Cells were maintained in t25 tissue culture flasks, kept in an incubator at 37°C and 5% CO_2. Cells were passaged once per every 3-4 days for normal maintenance, keeping confluence below 90%. Trypsin was used as the dissociation reagent in passage and all other transfers of adherent cells. Cells frozen for longer term storage were suspended in a ten percent DMSO and culture media solution, then transferred to 1mL cryogenic vials. The aliquots were then frozen at -80°C, housed in styrofoam to control freezing rate.

Cells to be transiently transfected were grown in t75 flasks to 80-90 percent confluency. Cells were then seeded on a six well plate, and incubated to 80 percent confluence. Qiagen Effectene® transfection reagent was then used to transfect cells with ligation products containing GFP-tagged protein, as described in the published protocol (36).

Detergent Fractionation

Following the execution of methods detailed by Baghirova et al. (37), cells were washed with phosphate buffered saline prior to trypsinization to detach cells. 5mL DMEM+5%FBS was then added and the cells centrifuged at 500x g for 10min. The supernatant was then aspirated and the cells resuspended in 500uL PBS before centrifugation at 500x g for 10min. The supernatant was then discarded and 400uL lysis buffer A added. The resulting solution was then incubated on an end-over-end rotator for 10min at 4 degrees C. The solution was then centrifuged at 2000x g for 10min and the supernatant stored (cytosolic fraction). 400uL lysis buffer was then added and the pellet resuspended by vortexing. The resulting solution was then

incubated on ice for 30min before centrifugation at 7000g for 10min. The resulting fraction was then collected (membrane bound organelle fraction). 400uL Buffer C was then added and the resulting mixture incubated on an end-over-end rotator for 30min at 4 degrees C. The resulting solution was then centrifuged at 7800x g for 10min and the supernatant collected (nuclear protein fraction).

Fluorescent Microscopy

Cells were seeded on a six-well plate, with the addition of circular coverslips. The cells were then transfected as previously described (38). After a 24 hour incubation period, media was removed and cells were washed in phosphate-buffered saline (PBS), prior to the addition of ER-Tracker™ Red (BODIPY™ TR Glibenclamide) dye, following the published protocol[8]. Following a second wash in PBS, 4 percent paraformaldehyde was used to fix cells. Mounted slides were stored at 4°C until imaging was performed via a deconvoluting confocal microscope.

Colocalization Analysis

Li's Intensity Correlation Analysis (ICA) was used to quantitatively assess colocalization. This method plots the intensity of each pixel on the Y axis against the covariance across the two channels, measured by multiplying the differences between two corresponding pixel intensities and their respective means (39). High relative intensities at the same location of each channel will be reflected by a positive result for that pixel, indicating possible colocalization. The intensity correlation quotient is the proportion of positive results, subtracted by 0.5. This results in a range of 0.5 (perfect colocalization) to -0.5 (zero colocalization).

Results

Creation of a Tetracycline Controlled Plasmid

Research on PCV1 VP3 has utilized transient transfection as a tool for studying its expression and selective apoptotic ability. Such an approach has proven effective for the mutational experiments conducted in the past, but yields itself to fluctuations in transfection efficiencies and subsequent protein expression. As a result, the protein of interest may be vastly overexpressed in cells that receive a greater DNA load while other cells may receive no DNA at all. As such, the creation of a stable H1299 cell line transfected with PCV1 VP3 was deemed a useful tool for normalizing transgenic DNA amounts and promoting high transgene expression. Through such a cell line, the implementation of subcellular studies such as fractionation would be greatly facilitated as low transfection efficiencies which may yield unusable samples could be avoided.

The major concern regarding a stable PCV1 VP3 transfection is the protein's apoptotic ability, since all transfected cells would shortly die if the transgene were "on" by default. To circumvent this, a Tet-On system was deemed ideal for inducible expression. This system, developed by modifying the Tet-off system found in nature, is "off" by default, with transcription allowed only in the presence of tetracycline. This allows researchers to induce expression and subsequent cell death when desired, preventing undesired transgene production and cell obliteration. Figure 1 details the mechanism by which this regulation system functions, whereby in the absence of tetracycline, the reverse tetracycline transactivator (rtTA) is unable to bind the tetracycline response element (TRE) (Figure 1A). The presence of tetracycline, however, causes a conformational change in the rtTA that allows it to bind the TRE and subsequently promote transcription (Figure 1B) (40). In order to implement this system, the pCW57.1 plasmid

(41) was selected from Addgene due to its incorporation of both the TRE and rtTA elements, making only one plasmid necessary (Figure 2A).

The protein of interest, PCV1 VP3 (conjugated to EGFP) was then cloned out of the pEGFP-C1 plasmid (Figure 2B) utilizing primers encompassing the entire protein complex, adding BmtI and AgeI restriction sites at the 5' and 3' ends respectively. This resulted in a 1.4kbp fragment (Figure 3A) which was purified from the gel. Both this product and isolated pCW57.1 were then digested with BmtI and AgeI and gel excised to yield the vector backbone containing the TRE promoter and rTetR (rtTA) (Figure 3B).

Following the successful creation and isolation of the vector backbone and the PCV1 VP3 insert, several ligation attempts were made utilizing T4 ligase to synthesize the desired plasmid (Figure 2C). Ligation products were then transformed into JM109 E.coli and grown under ampicillin selection, for which the pCW57.1 backbone provides resistance (not shown). All ligation attempts to date have failed to yield colonies following transformation and efforts to complete this construct are ongoing. Upon completion, this construct would function to achieve high expression levels and improve efficiency of the following subcellular localization studies. Additionally, by normalizing expression, transcriptome studies may also become possible and artifacts resulting from overexpression may be avoided.

Detergent Fractionation Subcellular Localization Studies

Previous studies have revealed PCV1 VP3 to be strongly cytoplasmic due to a strong NES in its tail region as exhibited by the cytoplasmic nature of the tail truncation. Interestingly, this truncation retains apoptotic ability while the core region, which retains high similarity to other apoptotic circovirus VP3s and is nuclear, does not. This indicates that PCV1 VP3's presence outside the nucleus may be critical to its apoptotic function, though its exact location

remains elusive. Due to this deviation in localization behavior as compared to other circovirus VP3s, PCV1 VP3 may likely have a distinct mechanism of action that has yet to be elucidated.

As exemplified by the PCV1 VP3 truncations themselves, a protein's subcellular localization can be critical to function. The compartments inside a cell are highly ordered, limiting what interactions a given molecule may undergo in any specific region. Through this principle, a protein's localization is likely highly relevant to its function, as is Apoptin's presence in the nucleus. Due to the difficulty in discerning PCV1 VP3's mechanism of action via truncation studies, studying its subcellular localization and determining where it acts may provide valuable insight towards narrowing the field of which cellular components the protein may interact with and, subsequently, how it achieves its selective apoptotic effect.

Given the relatively large size of H1299 nuclei as compared to the cell as a whole and the resolution limits of traditional light microscopy, PCV1 VP3's tendency to localize to any specific organelle has proven difficult to determine, even in cases where punctate expression patterns have been observed. Since it is unknown if the protein of interest is even localized to a specific organelle or is strictly cytoplasmic, differential detergent fractionation was conducted on transfected cells as described by Baghirova et al. H1299 cells transfected with PCV1 VP3 subjected to this protocol were treated with lysis buffers A, B, and C to yield cytoplasmic, organelle, and nuclear fractions respectively. Each lysis buffer was formulated to contain a characteristic detergent cocktail designed to dissolve their corresponding membranes. Treatments were conducted near freezing and lysis buffers were supplemented with a protease inhibitor cocktail to prevent sample degradation. As depicted by Figure 4A, this process consisted of subsequently incubating culture samples in these buffers and retrieving each fraction via centrifugation and supernatant collection. Untransfected cells were run as a negative

control along with cells transfected with the PCV1 VP3 “Core” (aa. 1-121) truncation, known to localize to the nucleus, as a positive control.

The resulting cytoplasmic, membrane-bound organelle, and nuclear fractions were then subjected to SDS-PAGE with plans for Western Blotting against GFP, as depicted by Figure 4B, to detect the transgene. Figure 5 shows such a preliminary PAGE gel containing all three fractions with stained protein, though the quality of these early samples are questionable given the apparent lack of nuclear protein. Blotting against GAPDH, SERCA2, and Lamin A/C respectively would also be conducted as validation for fraction identity and purity. As with the molecular cloning experiments, these investigations have yet to be completed. It is expected that upon successful fractionation and analysis, the data collected would indicate whether the PCV1 VP3 protein is truly localized to a membrane bound organelle. These results would then have implications in more focused localization studies such as the following ER colocalization experiments.

Endoplasmic Reticulum Colocalization Studies

Preliminary visual comparisons of the localizations of GFP-bound PCV1-VP3 with various organelle stains in existing literature were made to identify possible sites of localization. The endoplasmic reticulum was identified as one such potential site, given the similar envelope-like perinuclear localization pattern observed in many transfected cells.

To investigate this association, H1299 cells transfected with PCV1-VP3, along with the core truncation, were stained using ER-Tracker Red and fixed prior to confocal microscopy imaging. The core truncation functioned as a control; a predominantly nuclear localization with little overlap with the ER was expected to be observed. Images were assessed for overlap between the GFP and Texas Red fluorescence signals visually and using ImageJ. Cells

representing both previously observed punctate and diffuse localization patterns were identified for analysis.

The core truncation mostly exhibited an expected nuclear localization pattern (Figure 5), evidenced by overlap with DAPI (Figure 5B-D). GFP signal detected outside the nucleus was largely punctate, but some noticeable overlap with the ER was observed, shown by the yellow regions in the composite image (Figure 5D).

PCV1-VP3 showed inconsistent co-localization with ER, appearing to overlap significantly in a portion of cells exhibiting the diffuse localization pattern. One such example appears in figure 6A, where a high degree of overlap with ER signal was apparent. Interestingly, a region with punctate GFP expression at the left of the cell is present, and appears to have less significant overlap with ER, as suggested by the green, rather than yellow coloration of that area in the composite. This pattern appears throughout microscopy; None of the observed punctate cells displayed obvious co-localization between PCV1-VP3 and ER.

Figure 6B shows an instance of moderately punctate expression, where GFP signal is less evenly distributed outside the nucleus and many more pinpoint regions of high expression are present. As indicated previously, there also appears to be less overlap than what was observed in the diffusely expressing cell, with many more areas of isolated TexRed signal visible in the composite.

Figure 6C shows an example of a highly punctate expression pattern; many more isolated areas of high GFP signal are present, and are larger than the pinpoints found in figures 6A-B. Most strikingly, there is very little apparent overlap in the composite image, with little yellow coloration and many instances of dense GFP expression in areas with little ER stain.

A second visualization of the diffuse and punctate expression patterns from figure 6 is shown in Figure 8, with signal intensities of pixel plotted. Panels 1C and 2C show the results of

subtracting the lower intensity signal from the higher intensity signal in the diffuse and punctate cells, respectively. In a hypothetical cell with perfect colocalization, the result would be a completely flat plot, indicating each corresponding pixel has the same intensity value. This procedure produced a much flatter plot of the diffuse cell than the punctate cell, illustrating the much higher degree of signal overlap suggested in Figure 6.

Colocalization was investigated quantitatively in Figure 9 using Li's intensity correlation analysis. The shape of both sets of plots suggest colocalization appears to vary based on intensity; negative x-axis values indicating poor colocalization are less prevalent at very high and very low intensities. The latter may be a reflection of the significant noise observed throughout microscopy. The fact that both the punctate and diffuse cells exhibit roughly the same total degree of colocalization under this analysis (diffuse ICQ = 0.365, punctate ICQ = 0.347) points to a much higher degree of colocalization in the punctate cell than suggested by qualitative analysis, but could be a product of poor image quality.

Discussion

The abrupt end of this project caused by the closure of WPI's campus in response to the COVID-19 pandemic left much data to be collected, the nature of which can only be speculated. The molecular cloning and fractionation experiments in particular yielded little data as they were still in development. Ideally the tetracycline controlled plasmid would have been synthesized via ligation of the restricted pCW57.1 vector backbone and EFGP-PCV1 VP3 fragments. This would have been followed by selection in JM109 E.coli grown on ampicillin-LB plates, miniprep, and transfection into H1299 human non-small cell lung carcinoma cells with selection via puromycin resistance. At this point, a transgenic cell line containing the EGFP-PCV1 VP3 gene would have been established and been utilized in applications requiring high and relatively uniform expression rates within a cell culture.

Immediately, this transgenic cell line could be utilized to induce high PCV1 VP3 expression in cultures grown for fractionation. By eliminating the transfection step for expressing PCV1 VP3 in cell culture, this method would avoid potentially low transfection rates, instead producing expression in a majority of cells. While expression rates have yet to be observed under this system, it is not unreasonable to assume that, since every cell grown in this theoretical culture should contain the virus transgene, nearly every cell should produce the virus protein upon induction. By increasing expression efficiencies through this manner, samples produced for fractionation of any kind, including the detergent method followed in this project, would likely be of higher quality. This would be due to higher protein concentrations reducing the risk of false negatives in detection assays, such as the western blot method described previously.

A potentially even more valuable quality of the described transgenic cell line would be its propensity towards DNA normalization. Under transient transfection, cells are randomly imbued

with any copy number of the DNA vector, leading to fluctuations in expression. The same would theoretically occur as H1299 cells were transfected with the tetracycline controlled PCV1 VP3 plasmid, however the copy number would then likely stabilize around one through puromycin selection. This is because cells typically destroy forgein DNA, but under these conditions would require at least one transgene copy to survive.

The resulting DNA normalization could have important implications for the subcellular localization studies focused on in this project. Fluorescence microscopy experiments conducted here and in previous studies have observed both diffuse and punctate expression patterns of PCV1 VP3 in H1299 cells. Given the variable nature of transient transfection however, it is unclear if this is due to natural variation in protein expression or if this confounding observation is an artifact resulting from over expression in some cells. Utilizing this transgenic cell line could provide insight into this issue, since if this pattern is still observed under normalized conditions, it is likely a natural and potentially an important part of the protein's mechanism. If this pattern is an artifact of overexpression in some cells however, microscopy involving this transgenic cell line could determine if the protein's localization is primarily punctate or diffuse.

Excitingly, another opportunity that could be provided by DNA normalization is the potential for bioinformatics study. Transcriptomics, the study of which genes are active in a cell via RNA levels, has opened the door for determining changes in cell metabolism in response to stimuli. Among the most simple methods for studying which genes are being expressed through transcription are microarrays. Based on the hybridization of complementary sequences, RNA microarrays probe for specific nucleotide sequences corresponding to predetermined genes of interest which may be implicated in a biological pathway. As the knowledge base for human biological pathways has vastly increased, the opportunities and conveniences offered by this technique have grown, particularly with the creation of commercially available apoptosis specific

microarrays. Such assays test for families of genes known to participate in apoptosis, such as the caspase genes critical to Apoptin function which previous experiments have potentially implicated in PCV1 VP3 metabolism.

Microscopy failed to disprove colocalization between PCV1-VP3 and endoplasmic reticulum, but evidence in support of colocalization in only diffuse cells from quantitative methods was far weaker than qualitative investigation. The contradictory results obtained from colocalization microscopy highlight the need for further investigation, using a higher number and quality of cell images to confirm the relationship between expression pattern and degree of colocalization with ER. Future experiments may also control for cell cycle state and amount of PCV1-VP3 DNA, the latter being another strong application for the proposed stable cell line. The cell line may also facilitate in-vivo observation of colocalization, by introducing a live-cell ER-specific marker prior to activation of PCV1 VP3 expression. Coupled with cell cycle control, these results could yield new information concerning localization across cell lifetime. In any case, microscopy is not a tool that conclusively demonstrates colocalization when used alone, and is to be independently confirmed or disproved with alternative methods such as detergent fractionation.

If ER colocalization is demonstrated, investigation could shift to apoptosis pathways that implicate the endoplasmic reticulum, such as the unfolded protein response. Again, an inducible cell line for use with a microarray would be a valuable tool for investigating this narrowed-down group of pathways. Identifying the specific pathway used by PCV1-VP3 would be a critical step in development of novel therapies based on the action of circovirus proteins.

Figures

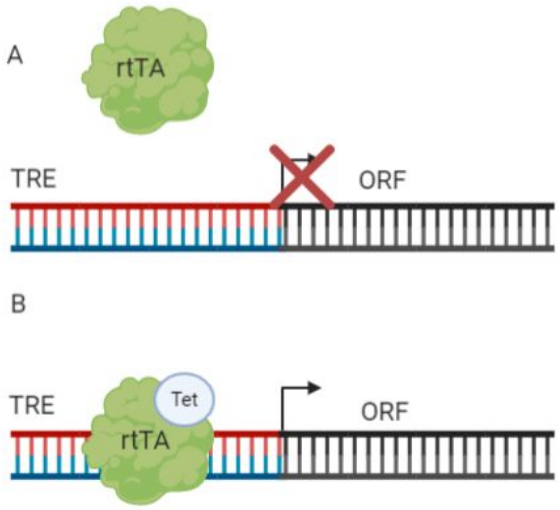

Figure 1. Tet-On Gene Regulation System. A. Reverse tetracycline transactivator (rtTA) in the absence of tetracycline does not bind the tetracycline response element (TRE) and the corresponding gene is not expressed. **B.** rtTA in the presence of tetracycline binds the TRE and promotes transcription.

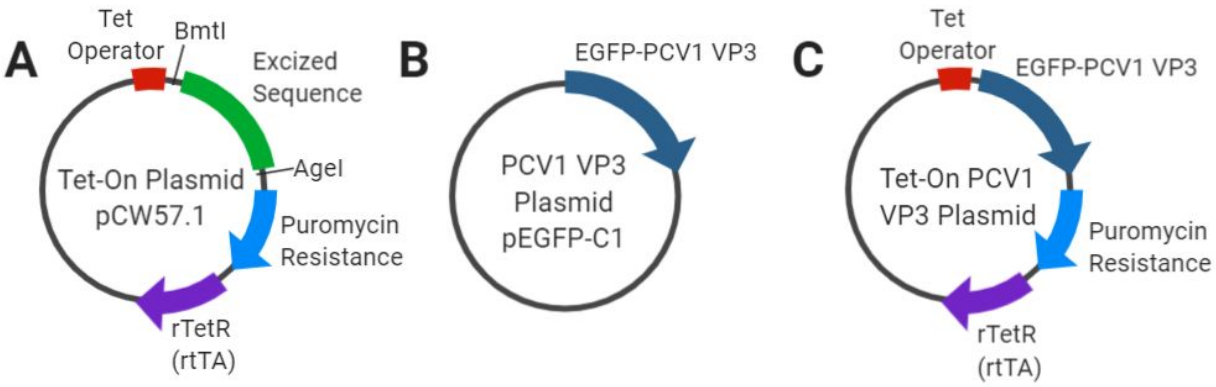

Figure 2. Plasmid Maps. A. Tetracycline controlled plasmid backbone containing both the Tet operator and the reverse tetracycline transactivator (rtTA). **B.** Plasmid containing the viral protein of interest PCV1 VP3 conjugated to EGFP. **C.** Synthesized plasmid consisting of the Tet controlled plasmid backbone and EGFP-PCV1 VP3.

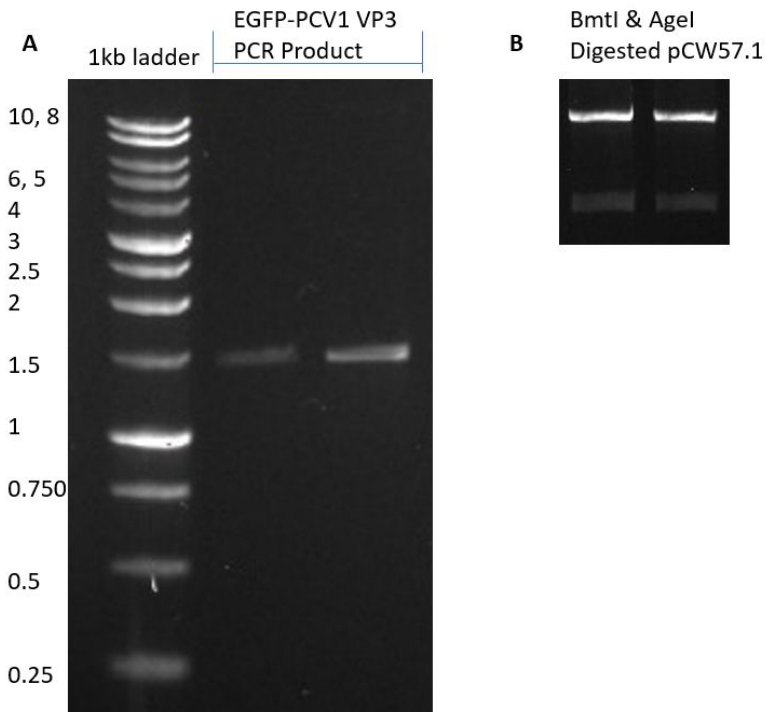

Figure 3. Molecular Steps for the Creation of a Tet-On PCV1 VP3 Plasmid. A. EGFP-PCV1 VP3 products after PCR with modified primers. **B.** Restriction digest products of pCW57.1 treated with both BmtI and AgeI reveal two bands corresponding to the tet vector backbone and an excised sequence (Figure 2A).

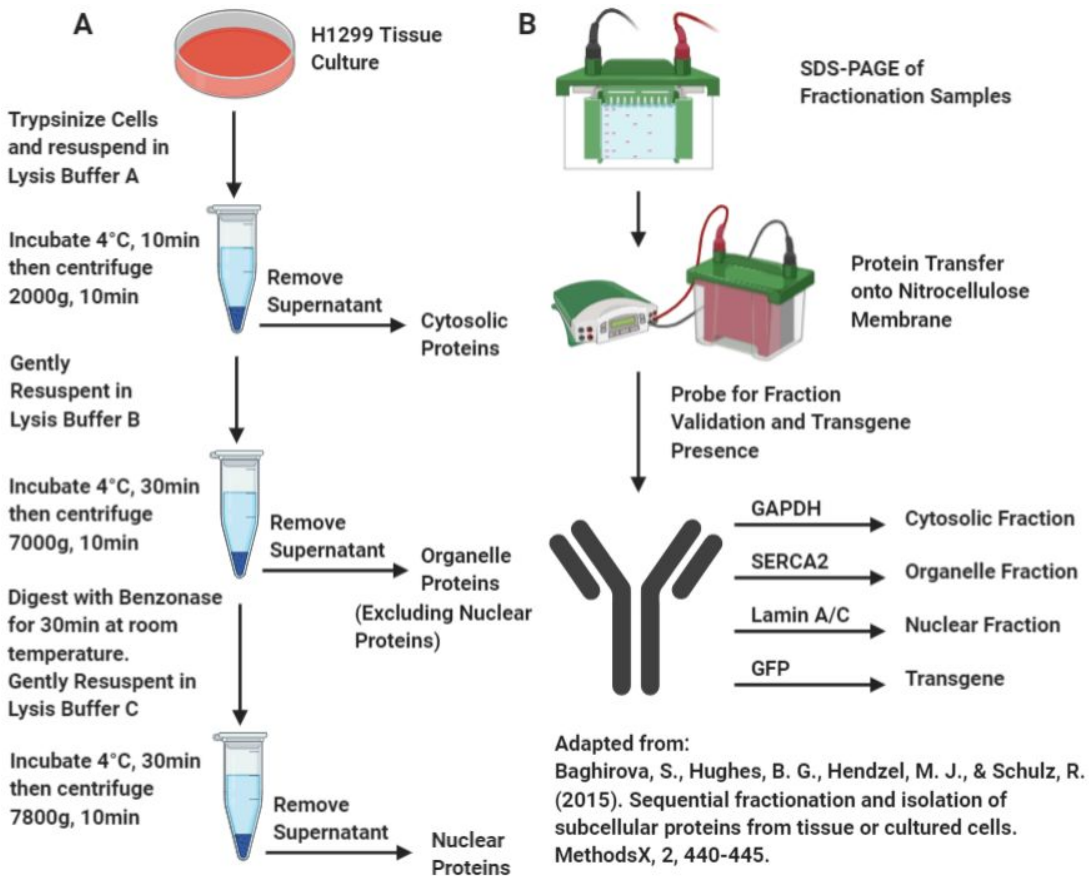

Figure 4. Differential Detergent Fractionation (DDF) and Analysis Procedure. A. Sequential detergent fractionation of cultured H1299 cells for yielding cytosolic, organelle, and nuclear fractions. **B.** Subsequent immunoblotting of culture fractions validating fraction identity and association with transgene.

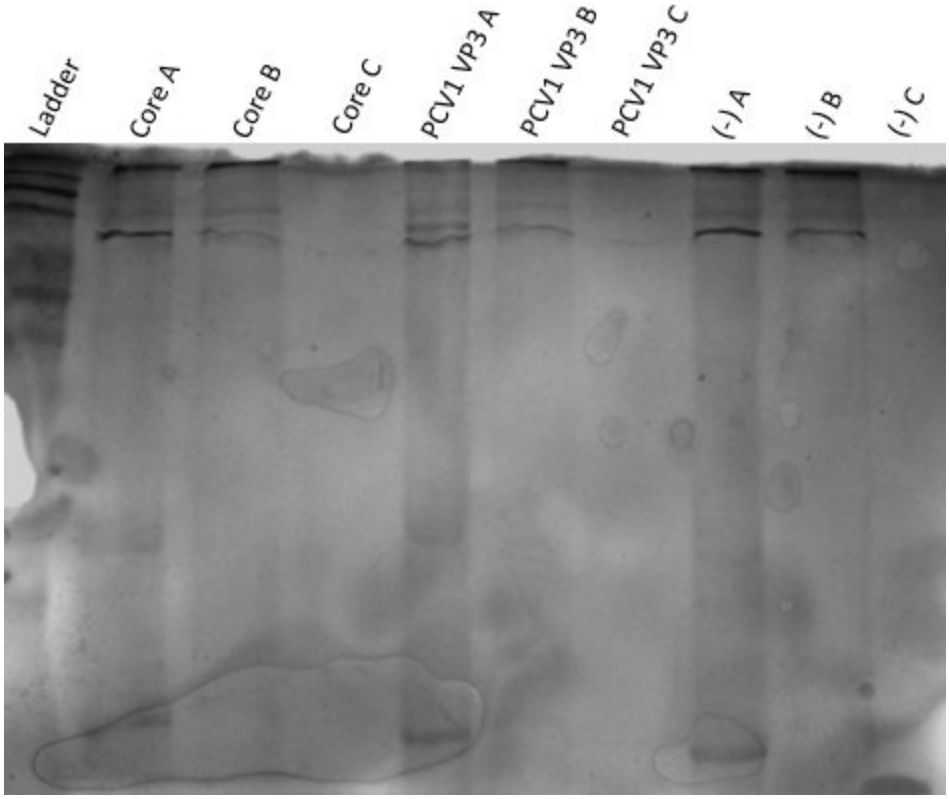

Figure 5. SDS-PAGE of DDF Samples. Preliminary gel of PCV1 VP3 and controls prior to Western Blotting. “Core” stands for the PCV1 VP3 core truncation reported to be nuclear and “(-)” stands for untransfected cells.

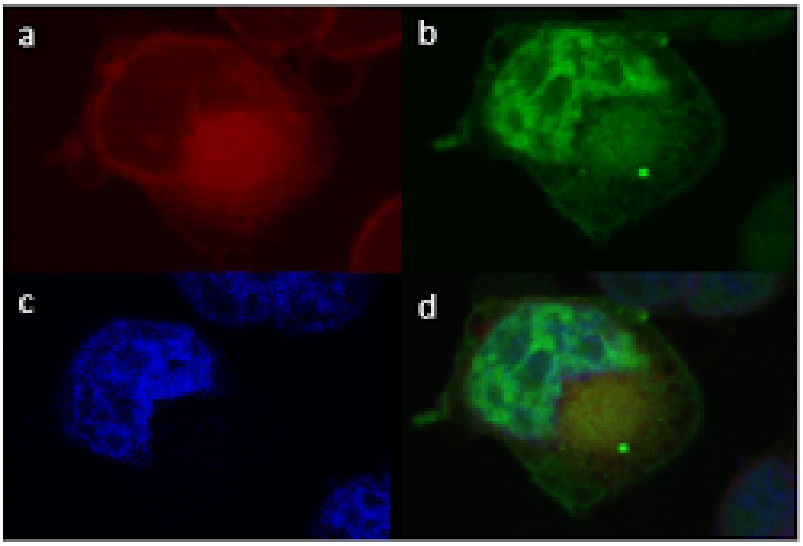

Figure 6. Representative Microscopic Images of PCV1 VP3 Core Truncation. A. ER stain excitation. **B.** GFP excitation. Truncation shows characteristic nuclear localization. **C.** Nuclear stain excitation. **D.** Composite of all three excitations.

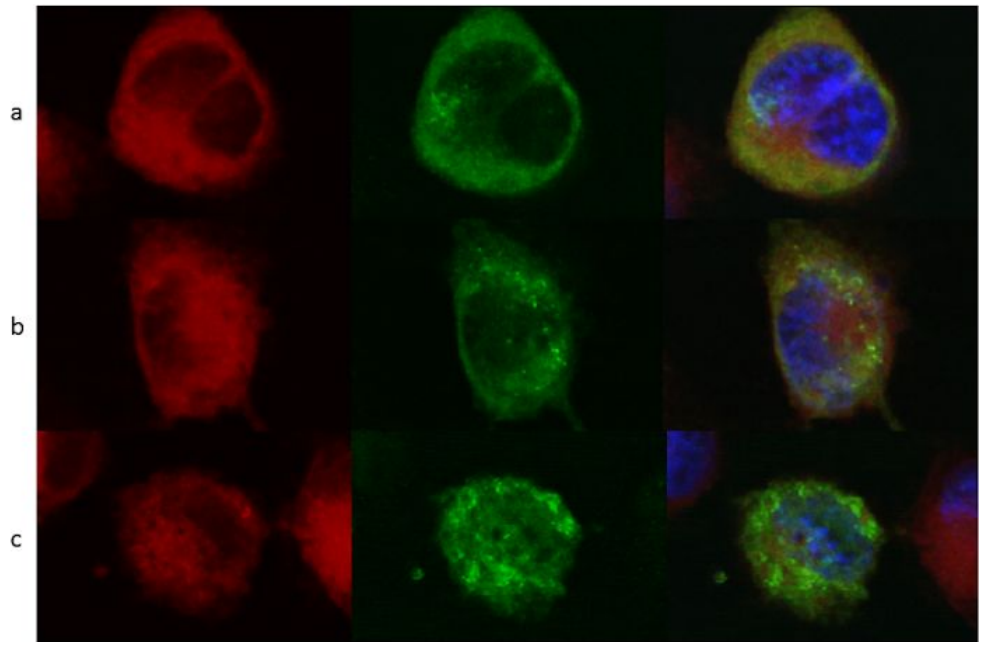

Figure 7. PCV1 VP3 Expression Patterns. Various expression patterns under ER stain excitation, GFP excitation, and a composite including nuclear stain (blue). Yellow indicates overlap between ER stain and GFP. **A.** Diffuse localization pattern. Noticeable overlap observed. **B.** Moderately punctate expression. Less overlap observed. **C.** Very punctate expression. Little to no overlap observed.

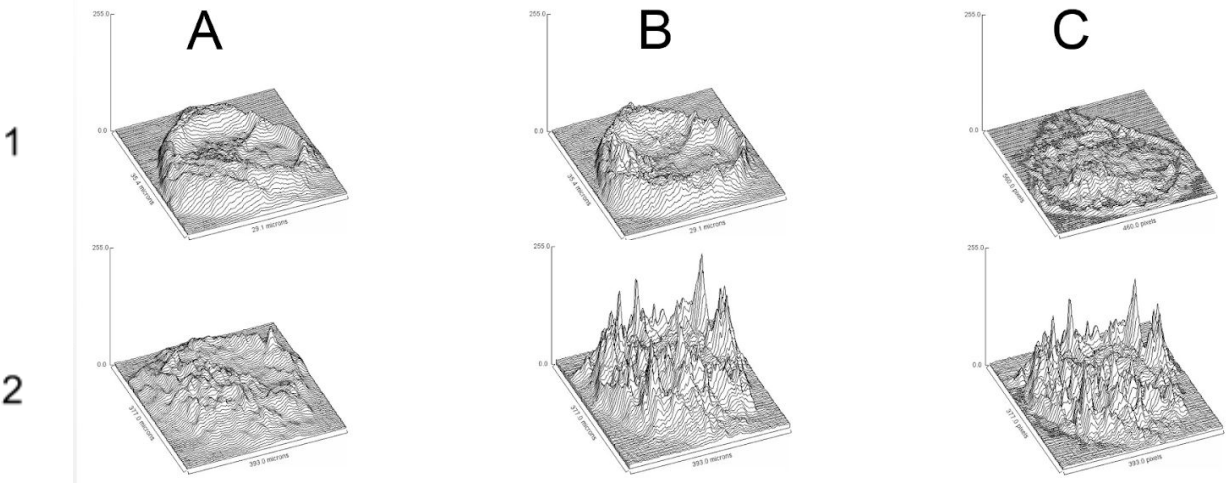

Figure 8. PCV1 VP3 Surface Plots. Visualization of (**A**) ER stain intensity and (**B**) GFP intensity measured from PCV1 VP3 microscopy in the diffuse (**1**) and punctate (**2**) expressers in figure 1. **C.** Appearance of overlap in the diffuse cell is highlighted by subtracting the GFP fluorescence intensity from ER stain fluorescence, yielding a much flatter result.

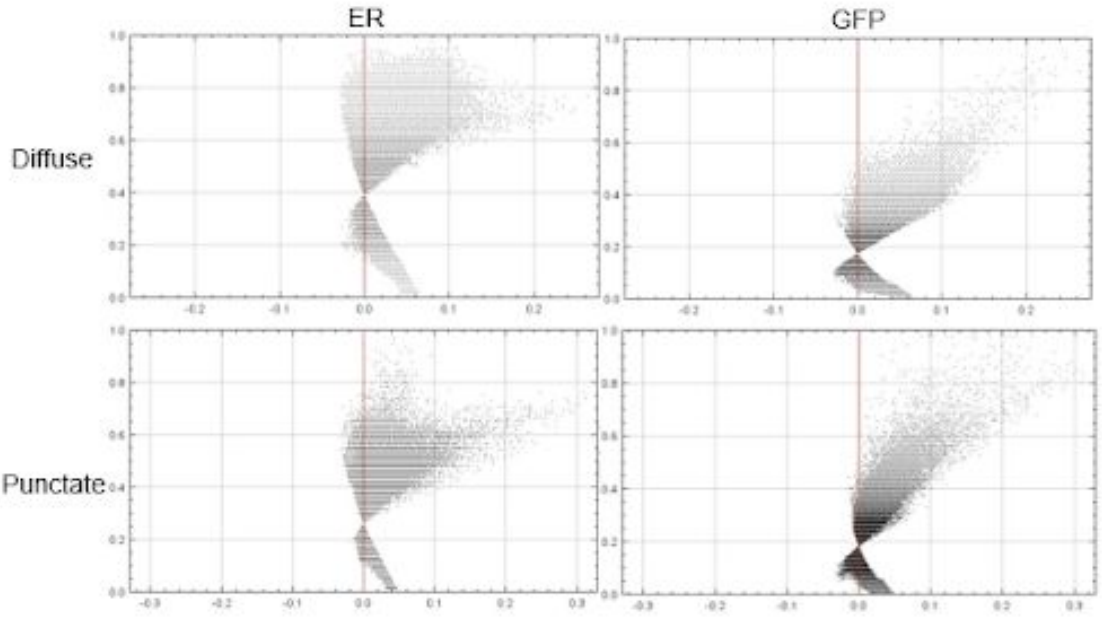

Figure 9. Li's Intensity Correlation Analysis. Intensity correlation plots for ER stain and GFP in diffuse and punctate expressers. Results indicate potential for colocalization in both expression patterns.

References

1. Zeng, S., Shen, W. H., & Liu, L. (2018). Senescence and Cancer. Cancer translational medicine, 4(3), 70–74. https://doi.org/10.4103/ctm.ctm_22_18
2. Baba AI, Câtoi C. Comparative Oncology. Bucharest (RO): The Publishing House of the Romanian Academy; 2007. Chapter 3, TUMOR CELL MORPHOLOGY. Available from: https://www.ncbi.nlm.nih.gov/books/NBK9553/
3. Zhou D, Luo Y, Dingli D, Traulsen A (2019) The invasion of de-differentiating cancer cells into hierarchical tissues. PLoS Comput Biol 15(7): e1007167. https://doi.org/10.1371/journal.pcbi.1007167
4. Bold, R., Termuhlen, P., & Mcconkey, D. (1997). Apoptosis, cancer and cancer therapy. Surgical Oncology, 6(3), 133–142. https://doi.org/10.1016/S0960-7404(97)00015-7
5. p53 Status and the Efficacy of Cancer Therapy in Vivo. (1994). Science, 266(5186), 807–810. https://doi.org/10.1126/science.7973635
6. Walboomers, J. M., Jacobs, M. V., Manos, M. M., Bosch, F. X., Kummer, J. A., Shah, K. V., ... & Muñoz, N. (1999). Human papillomavirus is a necessary cause of invasive cervical cancer worldwide. The Journal of pathology, 189(1), 12-19.
7. Marshall, E. (1999). Gene therapy death prompts review of adenovirus vector. Science, 286(5448), 2244-2245.
8. Breitbart, M., Delwart, E., Rosario, K., Segalés, J., Varsani, A., and ICTV Report Consortium. 2017, ICTV Virus Taxonomy Profile: Circoviridae, Journal of General Virology, 98: 1997–1998.
9. “Genus: Circovirus.” International Committee on Taxonomy of Viruses (ICTV), talk.ictvonline.org/ictv-reports/ictv_online_report/ssdna-viruses/w/circoviridae/659/genus-circovirus. Retrieved from: https://talk.ictvonline.org/ictv-reports/ictv_online_report/ssdna-viruses/w/circoviridae/659/genus-circovirus
10. King, A. M., Lefkowitz, E., Adams, M. J., & Carstens, E. B. (Eds.). (2011). Virus taxonomy: ninth report of the International Committee on Taxonomy of Viruses (Vol. 9). Elsevier.
11. Dane-Oorschot, A.A.A.M. van, et al. Apoptin Induces Apoptosis in Human Transformed and Malignant Cells but Not in Normal Cells. Jan. 1997.
12. Maddika, S., Mendoza, F. J., Hauff, K., Zamzow, C. R., Paranjothy, T., & Los, M. (2006). Cancer-selective therapy of the future: apoptin and its mechanism of action. Cancer biology & therapy, 5(1), 10-19.
13. Teodoro, J. G., Heilman, D. W., Parker, A. E., & Green, M. R. (2004). The viral protein Apoptin associates with the anaphase-promoting complex to induce G2/M arrest and apoptosis in the absence of p53. Genes & development, 18(16), 1952-1957.
14. Zhou, S., Zhang, M., Zhang, J., Shen, H., Tangsakar, E., & Wang, J. (2012). Mechanisms of apoptin-induced cell death. Medical oncology, 29(4), 2985-2991.

15. Olivier, M., Hollstein, M., & Hainaut, P. (2010). TP53 mutations in human cancers: origins, consequences, and clinical use. Cold Spring Harbor perspectives in biology, 2(1), a001008.
16. Peñaloza, O. M. R., Lewandowska, M., Stetefeld, J., Ossysek, K., Madej, M., Bereta, J., ... & Łos, M. J. (2014). Apoptins: selective anticancer agents. Trends in molecular medicine, 20(9), 519-528.
17. Chen, S., Li, Y. Q., Yin, X. Z., Li, S. Z., Zhu, Y. L., Fan, Y. Y., ... & Zhang, Q. G. (2019). Recombinant adenoviruses expressing apoptin suppress the growth of MCF‐7 breast cancer cells and affect cell autophagy. Oncology reports, 41(5), 2818-2832.
18. Phan, T. G., Giannitti, F., Rossow, S., Marthaler, D., Knutson, T. P., Li, L., ... & Delwart, E. (2016). Detection of a novel circovirus PCV3 in pigs with cardiac and multi-systemic inflammation. Virology journal, 13(1), 184.
19. Gagnon, C. A., Tremblay, D., Tijssen, P., Venne, M. H., Houde, A., & Elahi, S. M. (2007). The emergence of porcine circovirus 2b genotype (PCV-2b) in swine in Canada. The Canadian Veterinary Journal, 48(8), 811.
20. Lin, C., Gu, J., Wang, H., Zhou, J., Li, J., Wang, S., ... & Jiang, P. (2018). Caspase-dependent apoptosis induction via viral protein ORF4 of porcine circovirus 2 binding to mitochondrial adenine nucleotide translocase 3. Journal of virology, 92(10), e00238-18.
21. Liu, J., Chen, I., & Kwang, J. (2005). Characterization of a previously unidentified viral protein in porcine circovirus type 2-infected cells and its role in virus-induced apoptosis. Journal of virology, 79(13), 8262-8274.
22. Baker, K. M., & Gammal, R. S. (2010). Investigating the Ability of Porcine Circovirus 2 to Selectively Target and Kill Cancer Cells.
23. Teras, M., Viisileht, E., Pahtma-Hall, M., Rump, A., Paalme, V., Pata, P., ... & Boudinot, S. R. (2018). Porcine circovirus type 2 ORF3 protein induces apoptosis in melanoma cells. BMC cancer, 18(1), 1-12.
24. Zhang, Y., Sun, R., Geng, S., Shan, Y., Li, X., & Fang, W. (2019). Porcine circovirus type 2 induces ORF3-independent mitochondrial apoptosis via PERK activation and elevation of cytosolic calcium. Journal of virology, 93(7), e01784-18.
25. Allan, G. M., & Ellis, J. A. (2000). Porcine circoviruses: a review. Journal of Veterinary Diagnostic Investigation, 12(1), 3-14.
26. Hough, K. P., Rogers, A. M., Zelic, M., Paris, M., & Heilman, D. W. (2015). Transformed cell-specific induction of apoptosis by porcine circovirus type 1 viral protein 3. Journal of General Virology, 96(2), 351-359.
27. Rogers, A. M., Hough, K. P. (2012). The effect of subcellular localization on the oncoapoptotic capability of porcine circovirus type 1 VP3. WPI Project Reports.
28. Amato, K. (2016). Apoptotic Capabilities of Porcine Circovirus 1 Viral Protein 3 as a Function of Subcellular Localization. WPI Project Reports.
29. Clancey, S., Mahoney, B. (2013). Assessment of the Functionality of Nuclear Export Sequences in Porcine Circovirus 1 VP3. WPI Project Reports.
30. Mathur, A., Roy, T. (2015). Investigation of PCV1-VP3 Nuclear Export Signal Sequences Using Site-Directed Mutagenesis. WPI Project Reports.

31. Pakatar, N. (2015) Localization Assesment of Novel Nuclear Export Signal Sequence Mutants in PCV1-VP3.
32. Farris, L., Johnson, R. (2018). Analysis of Subcellular Localization of PCV1-VP3 Using Mutant Variants. WPI Project Reports.
33. Chaiyakul, M., Hsu, K., Dardari, R., Marshall, F., & Czub, M. (2010). Cytotoxicity of ORF3 proteins from a nonpathogenic and a pathogenic porcine circovirus. Journal of virology, 84(21), 11440-11447.
34. Promega Corporation. 2010. PureYield(TM) Plasmid Midiprep System Technical Manual, TM253.
35. Promega Corporation. 2009. Wizard SV Gel and PCR Clean-UP System Quick Protocol.
36. QIAGEN. 2002. Effectene® Transfection Reagent Handbook.
37. Baghirova, S., Hughes, B. G., Hendzel, M. J., & Schulz, R. (2015). Sequential fractionation and isolation of subcellular proteins from tissue or cultured cells. MethodsX, 2, 440-445.
38. Molecular Probes. 2005. ER-Tracker™ Dyes for Live-Cell Endoplasmic Reticulum Labeling.
39. Cordell F. 2008. JACoP v2.0: Improving the User Experience with Colocalization Studies. ImageJ User and Developer Conference.
40. T Das, A., Tenenbaum, L., & Berkhout, B. (2016). Tet-on systems for doxycycline-inducible gene expression. Current gene therapy, 16(3), 156-167.
41. pCW57.1 was a gift from David Root (Addgene plasmid # 41393 ; http://n2t.net/addgene:41393 ; RRID:Addgene_41393)